

Sulfide Capacity of High Alumina Blast Furnace Slags

AMITABH SHANKAR, MÄRTEN GÖRNERUP, A.K. LAHIRI, and S. SEETHARAMAN

Sulfide capacities of high alumina blast furnace slags were experimentally determined using the gas-slag equilibration technique. Two different slag systems were considered for the current study, namely, CaO-SiO₂-MgO-Al₂O₃ quaternary and CaO-SiO₂-MgO-Al₂O₃-TiO₂ quinary system. The liquid slag was equilibrated with the Ar-CO-CO₂-SO₂ gas mixture. Experiments were conducted in the temperature range of 1773 to 1873 K. The effects of temperature, basicity, and the MgO and TiO₂ contents of slags on sulfide capacity were studied. As expected, sulfide capacity was found to increase with the increase in temperature and basicity. At the higher experimental temperature, titania decreases the sulfide capacity of slag. However, at the lower temperature, there was no significant effect of titania on the sulfide capacity of slag. Sulfide capacity increases with the increase in MgO content of slag if the MgO content is more than 5 pct.

I. INTRODUCTION

THE concept of sulfide capacity was proposed by Fincham and Richardson,^[1] and it was defined as follows:

$$C_S = (\text{pct S}) \times \left(\frac{p_{\text{O}_2}}{p_{\text{S}_2}} \right)^{1/2} \quad [1]$$

In the last 50 years, there has been considerable research in the area of sulfide capacity of different slag systems. Several researchers^[1–6] have worked on the sulfide capacity of blast furnace slags. In spite of this, the literature review indicates that there is a lack of data for sulfide capacity of the CaO-SiO₂-MgO-Al₂O₃ slag system especially for high alumina slag with more than 15 pct alumina. Beside the experimental data reported on sulfide capacity, there are also some empirical models such as Young's model,^[6] Sommerville's model,^[7] and the KTH model,^[8] which predict the sulfide capacity of blast furnace slags very well within the domain of their investigation. Therefore, in the present work, the sulfide capacity of the CaO-SiO₂-MgO-Al₂O₃ and CaO-SiO₂-MgO-Al₂O₃-TiO₂ system was experimentally determined in the temperature range of 1773 to 1873 K.

II. EXPERIMENTAL

A. Materials

The materials used in the present work are listed in Table I. All the oxides were heated to 1273 K for 12 hours in a muffle furnace to remove any trace of moisture. Then, they were rapidly cooled and stored in desiccators.

B. Experimental Procedure

The experimental setup is shown in Figure 1. All the experiments were carried out in a horizontal tubular

resistance furnace where temperature can be maintained up to 1973 K. This furnace consists of an alumina tube having 1.2-m length and 0.058-m inner diameter. The even temperature zone was measured and it was found that, over a length of 0.2 m, the temperature variation was within ± 1 K. Two radiation shields made of alumina were also used to maintain the even temperature zone inside the furnace and they were placed 0.1 m away from the sample.

The furnace was controlled through a PID controller, 902 series, supplied by Eurotherm (Leesburg, VA). Two different sets of Pt 30 pct Rh-Pt 6 pct Rh thermocouples were used. One thermocouple was fixed close to the furnace heating element, just outside the furnace tube, which was used to control the furnace temperature. The other thermocouple was fixed just above the sample to measure the sample temperature.

A gas mixture consisting of Ar-CO-CO₂-SO₂ was used for equilibration with liquid slag. The furnace was heated to target temperature with argon gas flushing at a flow rate of 400 mL/min. Once target temperature was achieved, the gas atmosphere was changed to Ar-CO-CO₂-SO₂. Argon was introduced into the reaction tube. The gas flow rates of Ar, CO, CO₂, and SO₂ were kept at 200, 100, 80, and 20 mL/min, respectively, keeping the total gas flow rate at 400 mL/min. Gas flow rates of different gases were estimated so that partial pressure of oxygen inside the furnace could generally be maintained less than 10^{-7} atm. Partial pressure of various gaseous species at the experimental temperatures is given in Table I. Purity of gases used is shown in Table II. Gas flow rates were controlled using a Bronkhorst hi-tech mass flow meter (Keranova AB, Upplands Väsby, Sweden). A narrow alumina tube led the gas mixture directly to the vicinity of the sample, minimizing thermal segregation effects in the gas mixture due to density differences. All four gases were purified before they entered the furnace. The gas cleaning system for purification of the gases is shown in Figure 2. Argon gas was passed through the column of silica gel and Mg (ClO₄)₂ to remove traces of moisture. The CO₂ impurity was removed by passing the gas through a column of ascarite. The argon gas was further passed through copper and magnesium turnings at 773 K to remove traces of oxygen. The moisture and CO₂ impurity in the CO gas were removed, as in the case of Ar. The CO gas was further passed through copper at 773 K in order to remove traces of oxygen, by allowing it to react with CO over Cu turnings. The CO₂ gas was purified by passing it

AMITABH SHANKAR, Researcher, is with Research and Development, Tata Steel, Jamshedpur 831 003, India. Contact e-mail: amitabh.shankar@tatasteel.com MÄRTEN GÖRNERUP, Researcher, and S. SEETHARAMAN, Professor, are with the Department of Material Science and Engineering, Royal Institute of Technology Stockholm 100 44, Sweden. A.K. LAHIRI, Professor, is with the Department of Metallurgy, Indian Institute of Science, Bangalore 560 012, India.

Manuscript submitted January 11, 2006.

through silica gel and Mg (ClO₄)₂ to remove traces of moisture. The SO₂ gas was purified by passing it through silica gel twice.

Partial pressure of oxygen inside the furnace was maintained between 3.5×10^{-8} and 2.0×10^{-7} atm so that sulfur entered the slag in the form of sulfide instead of sulfate. Partial pressure of oxygen and sulfur in the gas mixture was calculated using Thermocalc (Stockholm, Sweden) with the SSUB3 database. To check the reliability and accuracy of the SSUB3 database, a comparison of partial pressures has been made between the data reported in the literature and those estimated by the preceding database. This calculation was carried out for a gas mixture of nitrogen, hydrogen, CO₂, and SO₂ and is shown in Table III. Table III shows the comparison of calculated values of p_{O_2} and p_{S_2} obtained from the preceding database and other software and databases. From Table III, it is clear that the estimated value of p_{O_2}/p_{S_2} is comparable to FACT and CSIRO databases, and the percentage deviation is within 10 to 17 pct.

Slag samples were prepared by mixing appropriate proportions of the reagents in the ball mill, followed by pressing it into small pellets of approximately 1.0 g. Platinum cups (made of 0.127-mm platinum foil, 99.9 pct (metal basis)) were used to hold the samples. These samples were kept on an alumina boat and pushed inside the furnace. Samples were kept inside the furnace for approximately

6 hours at the target temperature. The time required to achieve the equilibrium was established by comparing the equilibrium sulfur values with 6 and 15 hours duration, and equilibrium sulfur values were found to be very close to each other. Hence, for subsequent experiments, the equilibrium time for sulfur saturation in the slag was taken as 6 hours. After equilibration, the samples were pulled out toward the cold end of the furnace using the silica tube. Samples were taken out from the platinum crucibles and sent for chemical analysis. The practice of postexperimental analysis was followed for all samples. The chemical analysis of oxides was performed by a Spectro flame*

*SPECTRO FLAME is trademark of M/S Pectro Analytical GmbH, Kleve, Germany.

inductive plasma spectrometer. Sulfur analysis was performed using a LECO** combustion-infrared spectrometer.

**LECO is trademark of the LECO Corporation, St. Joseph, MI.

Table I. Oxides and Gases Used in the Present Work

Material	Purity	Supplier
Calcium oxide (CaO)	reagent plus, 99.9 pct	Sigma Aldrich, Munich, Germany
Silicon oxide (SiO ₂)	pro analyse grade, 99.5 pct	Alfa Aesar, Karlsruhe, Germany
Magnesium oxide (MgO)	pro analyse grade	Sigma Aldrich, Munich, Germany
Alumina (Al ₂ O ₃)	99.7 pct	Sigma Aldrich, Munich, Germany
Argon (Ar)	Argon plus, 99.99 pct	AGA Gas, Stockholm
Carbon monoxide (CO)	S grade	AGA Gas, Stockholm
Carbon dioxide (CO ₂)	S grade	AGA Gas, Stockholm
Sulphur dioxide (SO ₂)	S grade	AGA Gas, Stockholm

III. RESULTS AND DISCUSSION

Sulfide capacities of the CaO-SiO₂-MgO-Al₂O₃ and CaO-SiO₂-MgO-Al₂O₃-TiO₂ systems were measured. Eight different slag compositions were chosen for each system based on two different levels of MgO and four different levels of basicity. The range of MgO was between 2 and 10 pct, and the basicity ratio was between 0.7 and 1.25. All the experiments were carried out at three different temperatures: 1773, 1823, and 1873 K. The slag compositions used in the present investigation along with the basicity values (mass pct CaO/mass pct SiO₂) are shown in Table IV. The values of the sulfide capacities measured for these slags in the present investigation are also presented in the same table. It should be mentioned here that the chemical composition of slags mentioned in the discussion are post-experimental compositions only. Some of the experiments were repeated to ascertain the reproducibility of results. In order to ascertain the reliability of the data produced in the present work, some reference slags were prepared that have a composition very close to the blast furnace slags, as reported by Richardson and Fincham.^[1] A comparison for

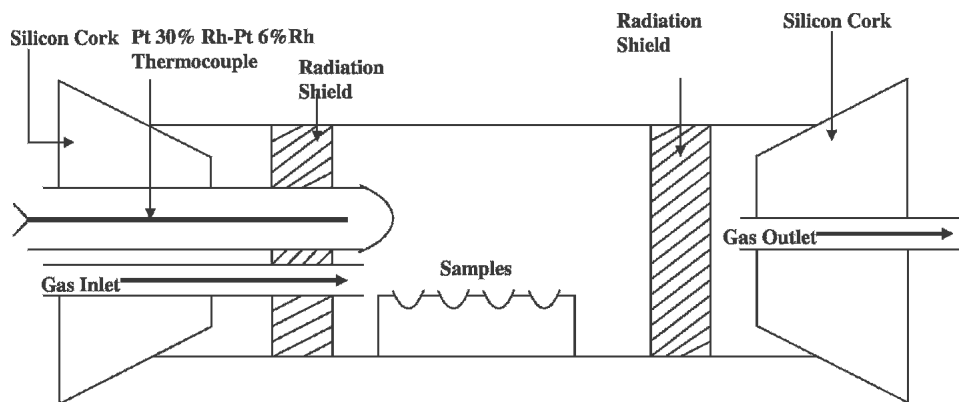


Fig. 1—Experimental setup for sulfide capacity.

Table II. Experimental Partial Pressure of Various Gaseous Species at the Experimental Temperatures

Species	Partial Pressure (Atm)		
	1773 K	1823 K	1873 K
Ar	$5.059 \cdot 10^{-1}$	$5.048 \cdot 10^{-1}$	$5.038 \cdot 10^{-1}$
CO	$2.043 \cdot 10^{-1}$	$2.117 \cdot 10^{-1}$	$2.185 \cdot 10^{-1}$
CO ₂	$2.499 \cdot 10^{-1}$	$2.418 \cdot 10^{-1}$	$2.343 \cdot 10^{-1}$
SO ₂	$2.568 \cdot 10^{-2}$	$2.918 \cdot 10^{-2}$	$3.234 \cdot 10^{-2}$
S ₂	$1.060 \cdot 10^{-2}$	$8.662 \cdot 10^{-3}$	$6.855 \cdot 10^{-3}$
O ₂	$3.560 \cdot 10^{-8}$	$8.759 \cdot 10^{-8}$	$2.061 \cdot 10^{-7}$

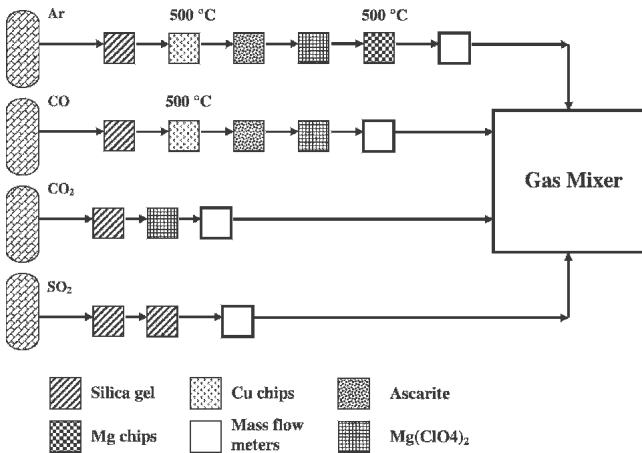


Fig. 2—Gas cleaning system for purification of gases.

Table III. Comparison of Calculated Values of p_{O_2} and p_{S_2} Obtained from Different Software and Databases

Software Database	Temperature (K)	p_{O_2}/p_{S_2}
FACT database	1773	$3.09 \cdot 10^{-3}$
CSIRO database	1773	$2.85 \cdot 10^{-2}$
Thermocalc (SSUB3 database)	1773	$3.47 \cdot 10^{-2}$

Gas Composition:
 $X_{N_2} = 0.5$, $X_{H_2} = 0.115$,
 $X_{CO_2} = 0.382$, and $X_{SO_2} = 0.003$

the preceding slag system has been made and is shown in Figure 3. It is clear from this figure that the results of the present work are in close agreement with the reported work, and deviation from the reported work lies in the range of 6 to 8 pct.

A. Effect of Basicity

Figure 4 shows the effect of basicity (mass pct CaO/mass pct SiO₂) on the sulfide capacity of the CaO-SiO₂-MgO-Al₂O₃ system with more than 20 pct alumina in the slag. Here, basicity was varied between 0.7 and 1.25 and the temperature between 1773 and 1873 K. It is evident from Figure 4 that, with the increase in basicity and temperature, the sulfide capacity of the slag increases. A similar observation was made by Xin and Chushao^[9] for the CaO-SiO₂-MgO-Al₂O₃-TiO₂ system and by Brown

Table IV. Chemical Compositions of the Slags Studied in the Present Work

Slag	CaO	SiO ₂	MgO	Al ₂ O ₃	TiO ₂	CaO/SiO ₂	T(°C)	$C_S \times 10^4$
S1	28.5	38.33	2.4	29.52	0	0.74	1500	1.136
S2	32.35	37.01	2	27.37	0	0.87	1500	1.89
S3	31.86	36.77	1.56	29.31	0	0.87	1500	1.67
S4	36.27	34.24	1.98	26.7	0	1.06	1500	3.15
S5	30.73	37.82	5.05	25.29	0	0.81	1500	1.32
S6	34.11	35.45	4.81	24.29	0	0.96	1500	2.53
S7	35.67	36.56	4.75	22.46	0	0.98	1500	2.603
S8	40.41	32.8	4.7	21.37	0	1.23	1500	5.66
SB1	29.8	37.73	2.55	29.5	0	0.79	1500	1.94
SB2	31.37	37.15	1.94	28.68	0	0.84	1550	3.117
SB3	34.6	36.38	4.92	23.67	0	0.95	1550	3.05
SB4	37.43	33.05	2.16	26.72	0	1.13	1550	5.058
SB5	29.05	39.79	4.96	25.52	0	0.73	1550	2.799
SB6	34.05	35.13	2.12	28.16	0	0.97	1550	4.01
SB7	33.41	37.66	4.49	23.79	0	0.89	1550	4.485
SB8	40.72	32.57	4.72	21.51	0	1.25	1550	9.26
SC1	28.61	37.85	2.63	29.32	0	0.76	1600	3.34
SC2	32.16	36.23	1.87	28.83	0	0.89	1600	4.88
SC3	32.55	35.17	2.75	28.46	0	0.93	1600	5.26
SC4	37.87	33.55	2.44	25.93	0	1.13	1600	8.66
SC5	31.01	38.94	5.56	24.42	0	0.8	1600	4.55
SC6	33.22	36.41	5.42	23.96	0	0.91	1600	6.03
SC7	34.68	36.07	4.75	22.97	0	0.96	1600	6.74
SC8	39.68	33.25	4.79	21.84	0	1.19	1600	14.25
T1	27.65	35.8	3.13	29.7	2.33	0.77	1500	1.08
T2	31.73	34.82	2.06	28.15	2.12	0.91	1500	2.15
T3	32.19	35.65	1.81	26.8	2.74	0.9	1500	1.27
T4	37.24	33.66	1.76	24.69	2.1	1.11	1500	3.48
T5	31.05	38.6	4.95	23.67	2.22	0.8	1500	2.05
T6	32.2	37.68	4.47	22.8	2.08	0.85	1500	2.01
T7	33.35	36	5.48	21.65	2.11	0.93	1500	3.34
T8	38.36	31.95	5.95	20.8	2.02	1.2	1500	5.26
T12	30.87	33.65	1.96	26.11	6.94	0.92	1500	2.16
T13	32.7	32.69	1.63	25.43	6.97	1.00	1500	2.58
T14	31.34	34.78	4.49	21.95	6.98	0.90	1500	2.68
T15	33.4	33.51	4.52	21.21	6.85	1.00	1500	3.35
TB1	27.1	36.63	2.62	30.26	2.45	0.74	1550	1.75
TB2	30.25	36.65	1.78	28.47	2.16	0.83	1550	2.99
TB3	32.63	34.17	2.2	27.48	2.47	0.95	1550	3.12
TB4	37.51	32.15	1.68	25.72	2.21	1.17	1550	5.12
TB5	29.54	37.5	5.4	24.43	2.31	0.79	1550	2.736
TB6	31.3	38.2	4.76	23.18	1.97	0.82	1550	3.913
TB7	34.26	35.66	4.73	22.4	2.32	0.96	1550	4.676
TB8	37.76	31.84	5.25	21.76	2.36	1.19	1550	7.889
TC1	27.29	36.44	2.77	30.06	3.05	0.75	1600	2.91
TC2	30.73	34.12	2.37	26.65	2.06	0.9	1600	5.044
TC3	32.09	34.76	2	26.74	2.59	0.92	1600	5.43
A1	32.14	37.43	9.6	18.66	0	0.86	1500	3.1
A2	35.44	34.3	6.42	21.58	0	1.03	1500	4.12
A3	34.1	34.66	7	20.3	0	0.98	1500	4.14

et al.^[10] for the CaO-SiO₂-MgO-TiO₂ and CaO-SiO₂-Al₂O₃-TiO₂ systems. At lower basicity, the CaO content in the slag is less, so that only a few free O²⁻ ions exist. This results in low sulfur distribution ratios and low sulfide capacities of slags. As the basic oxide contents increase, the SiO₂ networks are broken into smaller anion groups and the proportion of free oxygen ions increases. Consequently, the sulfur distribution ratio and sulfide capacity of slag are expected to increase. The effect of TiO₂ will be discussed in Section III-D.

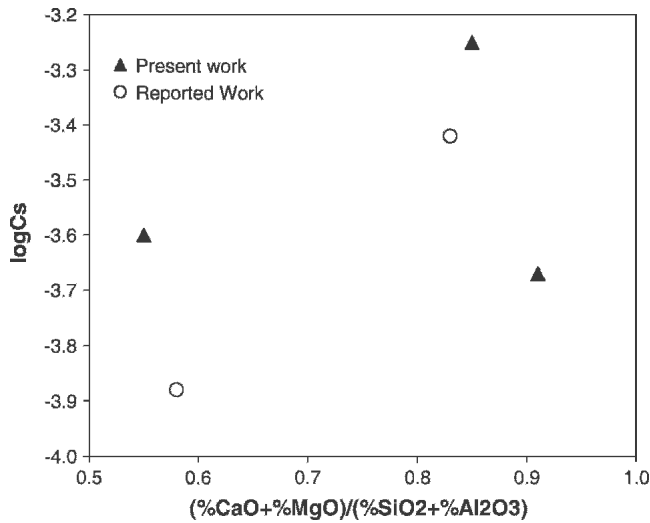


Fig. 3—Comparison of sulfide capacity of present work and reported work.

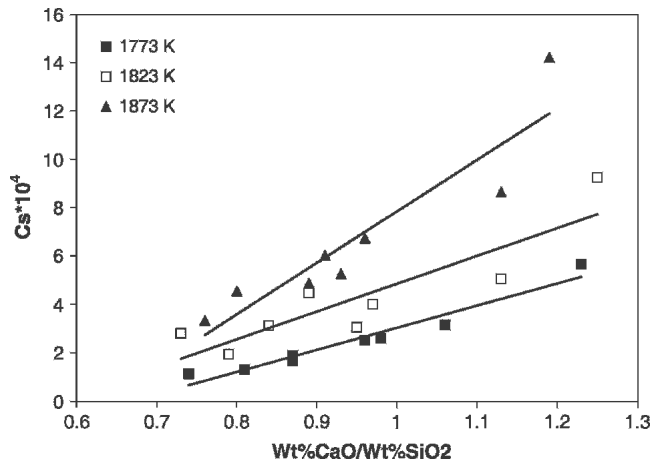


Fig. 4—Effect of basicity on sulfide capacity (C_S) of CaO-SiO₂-MgO-Al₂O₃ slags.

B. Effect of Temperature

In the present work, the effect of temperature on the sulfide capacities of slags of constant composition was examined. The sulfide capacities were found to increase with increasing temperature, which would be in accordance with the increase of free oxygen ions due to the breaking of the bonds. It would be interesting to examine the slope of the plots of $\log_{10} C_S$ vs $10^4/T$ in the case of the slags studied in the present work and to compare these with the experimental observations of other investigations reported in the literature for similar slags. Figure 5 shows the slope of $\log_{10} C_S$ vs $10^4/T$ for different slag systems. In the present work, the slope for the CaO-SiO₂-MgO-Al₂O₃ slag system was found to be 1.4, as opposed to the value of 1.2 found by Richardson and Fincham.^[1]

In the case of the binary system FeO-SiO₂, Richardson and Fincham^[1] as well as Mselly *et al.*^[11] carried out sulfide capacity measurements in the temperature range 1623 to 1873 K. The plot of $\log_{10} C_S$ vs $10^4/T$, presented in Figure 5, carried

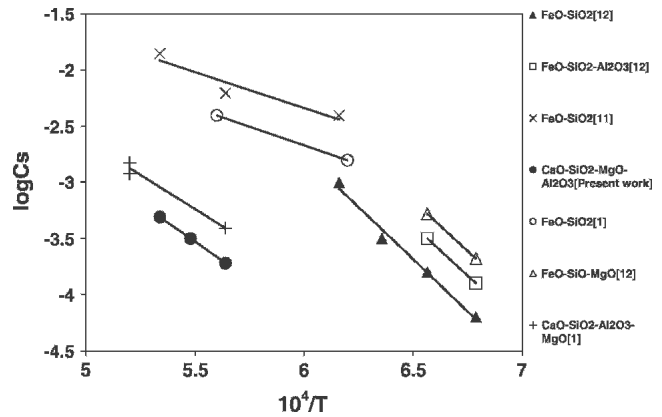


Fig. 5— $\log_{10} C_S$ vs $1/T$ curve for different slag systems.

out by the preceding authors shows that the curve is linear and the slope is 0.64. The sulfide capacities of this system have also been examined by Simeonov *et al.*,^[12] but at lower temperatures, *viz.* 1473 to 1623 K. These authors have also measured the sulfide capacities of the ternary systems FeO-SiO₂-Al₂O₃ and FeO-SiO₂-MgO in the same temperature range. It is significant that the slope of the $\log_{10} C_S$ vs $10^4/T$ was 1.86 for both binary and ternary systems. It is interesting to note in Figure 5 that the plots of $\log_{10} C_S$ vs $10^4/T$ for all the “FeO” containing slags show higher slope values at lower temperatures and *vice versa*. On the other hand, the results of the present measurements in the case of the system CaO-SiO₂-MgO-Al₂O₃ show that the slope is closer to the value for “FeO”-containing systems at lower temperatures. It was observed that FeO-containing slag systems have higher sulfide capacity compared to the non-FeO slag system. This is because FeO acts as a basic oxide, and the optical basicity of the former slag system is greater compared to the later slag system. A discussion of the effect of optical basicity on the sulfide capacity of the slag is presented at a later part of the present article. A more detailed study of the slopes of the $\log_{10} C_S$ vs $10^4/T$ plots is currently being carried out and will be presented in a separate publication.

C. Estimation of Slope of $\log_{10} C_S$ vs $10^4/T$ Curve

In the following section, a semiempirical correlation between the chemistry of the slag system and the slope of the $\log_{10} C_S$ vs $10^4/T$ plot is attempted.

For the slag system having one basic oxide, sulfur removal takes place per the following reaction:



The standard Gibb's free energy for the preceding reaction is

$$\Delta G^0 = \Delta H - \Delta S \times T \text{ (J/mol)} \quad [3]$$

$$\text{Further, } (\Delta G^0 = -RT \ln K \text{ (J/mol)}) \quad [4]$$

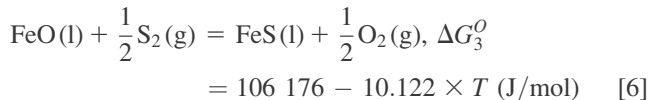
Using Eqs. [1] through [4],

$$\log C_S = -0.517 \times 10^{-5} \times \Delta H \left(\frac{10^4}{T} \right) + 0.0517 \times \Delta S + \log \left[(\text{pct S}) \frac{\gamma_{\text{MO}} \times X_{\text{MO}}}{\gamma_{\text{MS}} \times X_{\text{MS}}} \right] \quad [5]$$

In the preceding equation, it was assumed that ΔH , ΔS , γ_{MO} , and γ_{MS} are constant for the range of temperatures investigated in the present work.

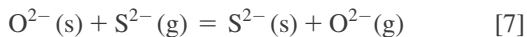
Hence, from Eq. [5], the slope of $\log C_S$ vs $10^4/T$ curve can be estimated.

For the FeO-SiO₂ system, sulfur removal takes place per the following reaction:

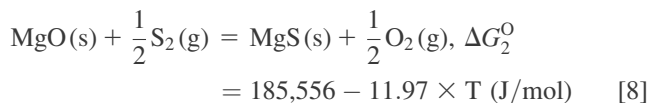


From Eq. [5], the slope was found to be 0.55, which is very close to the slope value reported by Mselly^[11] and Richardson^[1] for the FeO-SiO₂ system. For the same slag system, Simeonov *et al.*^[12] reported a higher value of the slope at the low-temperature region. A simple analysis reveals that the $\gamma_{\text{MO}}/\gamma_{\text{MS}}$ ratio increases with the decrease in temperature. Therefore, it can be said that the $\gamma_{\text{MO}}/\gamma_{\text{MS}}$ ratio will not be constant, especially at very low temperature. The fact that theoretical estimation of the slope does not match the results of Simeonov *et al.*^[12] is, in fact, attributed to the effect of temperature. A similar observation was found in the case of the FeO-SiO₂-Al₂O₃ system.

For any slag system having more than one basic oxide, sulfur removal will take place per following reaction:

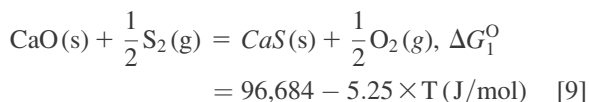


In the case of the FeO-SiO₂-MgO system, sulfur removal will take place per Reaction [6] as well as the following reaction:



For the preceding slag system, the slope of the $\log_{10} C_S$ vs $10^4/T$ curve was estimated from both Reactions [6] and [8]. These slopes were 0.55 and 0.96, respectively, for Reactions [6] and [8]. The sum of these two slopes is 1.51, which incidentally is close to the value of 1.86 estimated from the results of Simeonov *et al.* The lower value of the theoretical slope indicates that the ratio of the activity coefficients of oxides to sulfides is influenced by temperature, which was observed in the case of the binary slag system discussed earlier.

For the CaO-SiO₂-MgO-Al₂O₃ system, sulfur removal will take place per Reaction [8] and the following reaction:



For the preceding slag system, the slope was estimated from both Reactions [8] and [9]; these slopes were 0.5 and

0.96. The sum of these slopes is 1.46, which is very close to the experimental value 1.4 of the slope, as estimated from the $\log_{10} C_S$ vs $10^4/T$ curve. A similar observation was made for the FeO-SiO₂-MgO system. Therefore, it can be said that for the slag system having more than one basic oxide, the slope of the $\log_{10} C_S$ vs $10^4/T$ curve can be estimated by taking care of the enthalpies of all of the reactions involved in sulfur removal.

From the preceding analysis of the $\log C_S$ vs $10^4/T$ curve, it is possible to estimate the enthalpy of the desulfurization reaction, and it was calculated for some of the slag systems and a comparison was made. For the FeO-SiO₂ system, the enthalpy value was estimated and it was 123,791 J/mole for the desulfurization reaction, which is higher than the actual value. If the enthalpy value for the concerned desulfurization reaction is known, it should be possible to monitor the sensitiveness of sulfide capacity with respect to temperature, which is very important.

For the CaO-SiO₂-MgO-Al₂O₃ system, the enthalpy value was also estimated for the overall reaction responsible for desulfurization and it was 282,398 J/mole. This value matched well with the actual value. It can be seen that the enthalpy value for this slag system is higher than the FeO-SiO₂ slag system, which indicates that the sulfide capacity of the blast furnace slag is more sensitive to temperature than the FeO-SiO₂ slag system.

D. Effect of TiO₂

The effect of TiO₂ on the sulfide capacity of slags is shown in Figures 6 and 7. It seems from Figures 6 and 7 that TiO₂ does not have any significant effect on sulfide capacity at 1773 K. However, at 1873 K, there is a significant decrease in sulfide capacity with the increase in TiO₂. Therefore, it is possible to use titania (approximately 2 pct) in blast furnace slag at 1773 K to maintain same sulfide capacity and at the same time to improve other slag characteristics such as viscosity. In basic slags, TiO₂ exists as TiO₆⁸⁻ ions, which was confirmed by Sommerville and Bell.^[13] Therefore, TiO₂ in slag forms anions, which will cause free O²⁻ ions to decrease. In other words, higher the TiO₂ in the slag, the lower will be sulfide capacity. Similar work for blast furnace slags was also performed by Tang and Xu,^[9] where they have observed that, with the increase of 5 pct TiO₂ in the slag, sulfide capacity of slag decreases up to 25 pct TiO₂ at 1773 K.

E. Effect of MgO

Figure 8 shows the effect of MgO on the sulfide capacity of slags. It is evident from Figure 8 that there is no substantial effect of MgO on sulfide capacity if it increases from 2 to 5 pct. However, sulfide capacity increases with MgO if MgO increases to 7 pct or more. This occurs because effective basicity increases with the increase in MgO content, and this increase in basicity is significant above 5 pct MgO.

F. Effect of Optical Basicity

The concept of optical basicity was developed by Ingram and Duffy^[14] and was defined as follows:

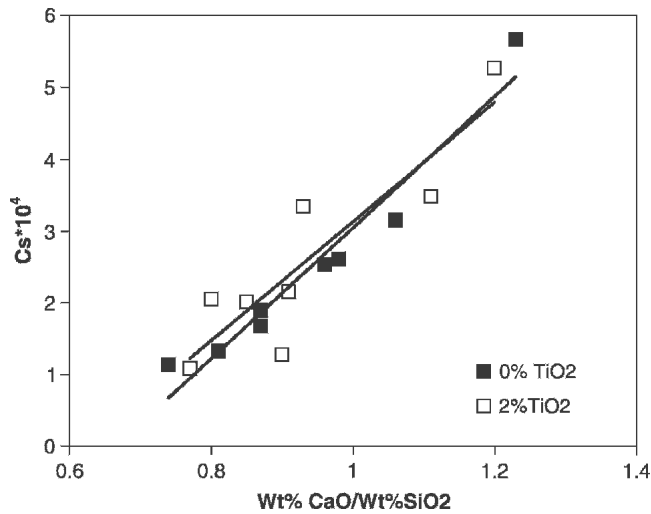


Fig. 6—Effect of TiO₂ on sulfide capacity (C_s) of CaO-SiO₂-MgO-Al₂O₃ slags at 1773 K.

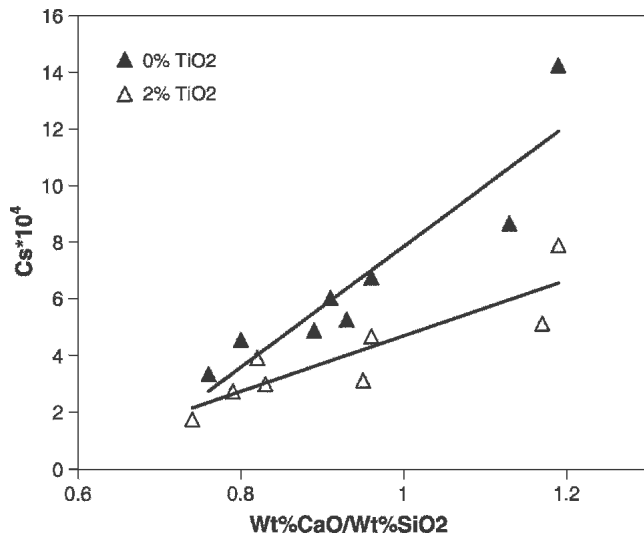


Fig. 7—Effect of TiO₂ on sulfide capacity (C_s) of CaO-SiO₂-MgO-Al₂O₃ slags at 1873 K.

$$\Lambda = \frac{\sum(X_i n_i \Lambda_i + \dots)}{\sum(X_i n_i + \dots)} \quad [10]$$

Optical basicity was used to relate the slag composition and the sulfide capacity of slag, first by Sosinsky and Sommerville^[7] and later by Young *et al.*^[6] They found a strong correlation between optical basicity and sulfide capacity. Therefore, a plot of the sulfide capacity as a function of optical basicity is plotted for the slag system of the present work and is shown in Figure 9. From the figure, it can be seen that sulfide capacity and optical basicity also have a good correlation for the high alumina slag system investigated in the present work, which is high alumina blast furnace slag.

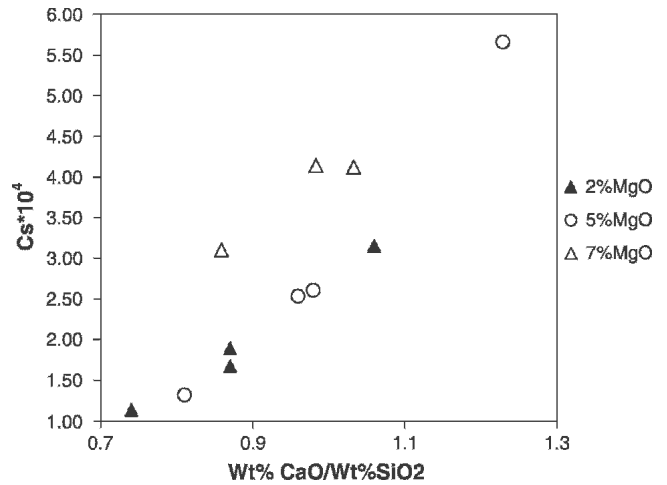


Fig. 8—Effect of MgO on sulfide capacity (C_s) of CaO-SiO₂-MgO-Al₂O₃ slags at 1773 K.

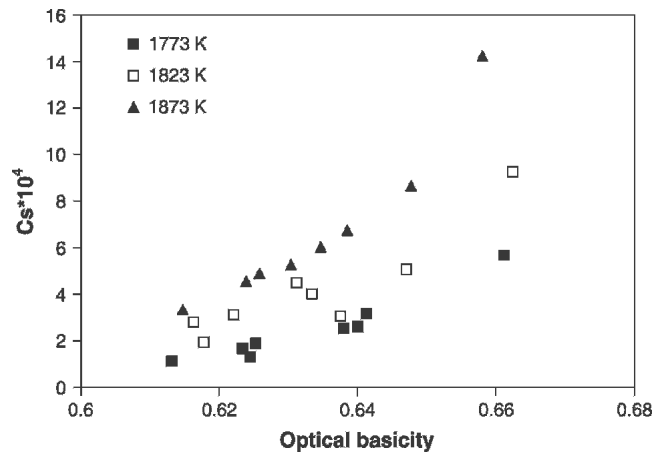


Fig. 9—Effect of optical basicity on sulfide capacity (C_s) of CaO-SiO₂-MgO-Al₂O₃ slags.

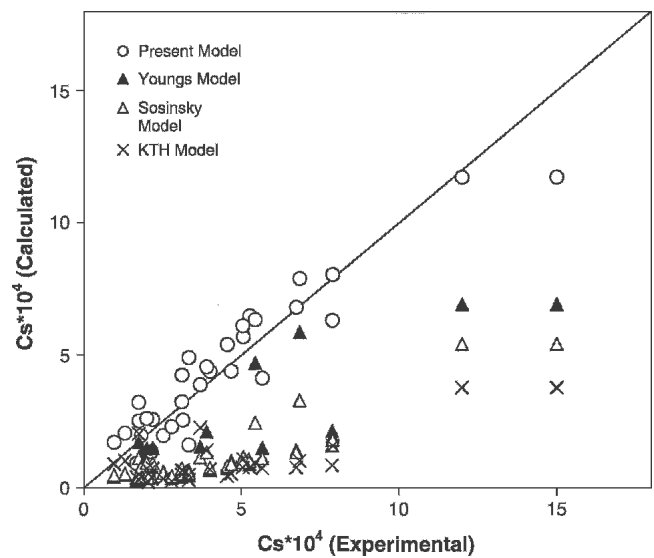


Fig. 10—Comparison between estimated and measured sulfide capacity (C_s) for CaO-SiO₂-MgO-Al₂O₃ system.

IV. MODELING OF SULFIDE CAPACITY

A comparison of experimental values of sulfide capacity along with the estimated values of sulfide capacity by Young's model,^[6] Sommerville's model,^[7] and the KTH model^[8] is shown in Figure 10. It is evident from Figure 10 that Young's model, Sommerville's model, and the KTH model underpredict the values of sulfide capacity. This may be because these models had been tuned for the low alumina slags. Therefore, a new model based on optical basicity has been proposed for high alumina slags, and it is shown in Eq. [11]. Prediction of sulfide capacity by this model is shown in Figure 10. It is clear from Figure 10 that this model estimates sulfide capacity very well for the present slag system as compared to other models. This model was also tested against the reported data of blast furnace slags, and this comparison is shown in Figure 11. From this figure, it is clear that prediction by this model is in close agreement with the reported data. The average deviations from the experimental value were 24 and 29 pct, respectively, for the present work and the reported work as opposed to 80 pct for the other reported models discussed in this article.

$$C_s = 9.852 \times 10^{-6} \times (\text{pct Al}_2\text{O}_3) + 0.010574 \times \Lambda - 16.2933 \times \frac{1}{T} + 0.002401 \quad [11]$$

The preceding equation has been developed for slags having CaO: 30 to 46 pct, SiO₂: 30 to 40 pct, MgO: 2 to 10 pct, Al₂O₃: 12 to 30 pct, and CaO/SiO₂: 0.74 to 1.4. The data used for developing the model is shown in Table IV. A total of 41 data were used for regression, and the correlation coefficient was 0.93. Further, the preceding model has been developed for slags having optical basicity between 0.63 and 0.70 and sulfide capacity between 1.0 and 9.0 × 10⁻⁴. The preceding range of optical basicity and sulfide capacity is very common for most of the blast furnace slag systems reported in the literature.^[1,2,9,16]

V. CONCLUSIONS

In the present work, sulfide capacities of the quaternary system CaO-SiO₂-MgO-Al₂O₃ system and the quinary system CaO-SiO₂-MgO-Al₂O₃-TiO₂, at selected temperature and composition, were experimentally measured using the gas-slag equilibration technique. These measurements were made with respect to basicity, MgO, and TiO₂ content. Sulfide capacity increases with the increase in basicity. The MgO increases the sulfide capacity of slag beyond the 5 pct level. At high temperature, TiO₂ affects the sulfide capacity of slag, and there is a decrease in sulfide capacity with the increase in TiO₂ content. On the basis of the preceding experimental data on sulfide capacity, an empirical model was developed for prediction of the sulfide capacity of high alumina slag systems. This model estimates the sulfide capacity well for the blast furnace type slags.

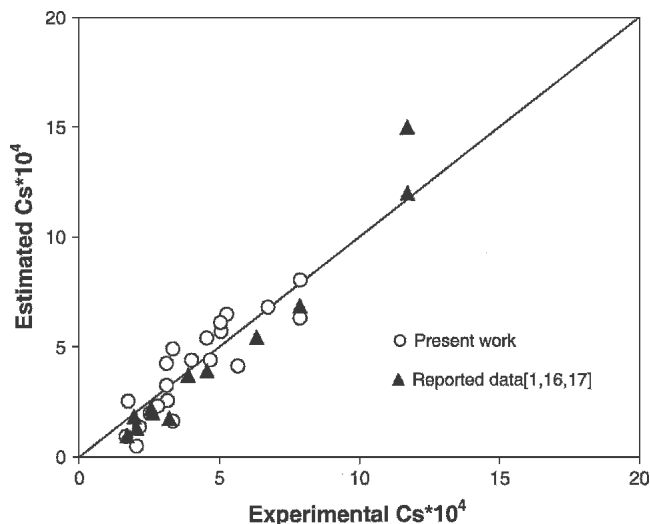


Fig. 11—Comparison between estimated and measured sulfide capacity of the reported work and the present work for the blast furnace slag.

LIST OF SYMBOLS

C_s	sulfide capacity
(pct S)	wt pct sulfur in slag
p_{O_2}	partial pressure of oxygen
p_{S_2}	partial pressure of sulfur
Λ_i	optical basicity
X_i	mole fraction
n_i	number of oxygen atoms

REFERENCES

1. F.D. Richardson and C.J.B. Fincham: *J. Iron Steel Inst.*, 1954, vol. 178, pp. 4-15.
2. K. Kärsrud: *Scand. J. Metall.*, 1984, vol. 13, pp. 173-75.
3. I. Ghita and H.B. Bell: *Ironmaking and Steelmaking*, 1982, vol. 9 (6), pp. 239-43.
4. K. Kärsrud: *Scand. J. Metall.*, 1984, vol. 13, pp. 265-68.
5. V.S. Venkatadri and S.K. Gupta: *Trans. Indian Inst. Met.*, 1979, vol. 32 (3), pp. 235-38.
6. R.W. Young, J.A. Duffy, G.J. Hassall, and Z. Xu: *Ironmaking and Steelmaking*, 1992, vol. 19 (3), pp. 201-19.
7. D.J. Sosinsky and I.D. Sommerville: *Metall. Trans. B*, 1986, vol. 17B, pp. 331-37.
8. M.M. Nzotta, D. Sichen, and S. Seetharaman: *Iron Steel Inst. Jpn.*, 1998, vol. 38 (11), pp. 1170-79.
9. T. Xin and X. Chushao: *Iron Steel Inst. Jpn. Int.*, 1995, vol. 35 (4), pp. 367-71.
10. S.D. Brown, R.J. Roxburgh, I. Ghita, and H.B. Bell: *Ironmaking and Steelmaking*, 1982, vol. 9 (4), pp. 163-67.
11. M.M. Nzotta, D. Sichen, and S. Seetharaman: *Iron Steel Inst. Jpn.*, 1999, vol. 39 (7), pp. 1657-63.
12. S.R. Simeonov, R. Sridhar, and J.M. Toguri: *Metall. Trans. B*, 1995, vol. 26B, pp. 325-34.
13. I.D. Sommerville and H.B. Bell: *Can. Metall. Q.*, 1982, vol. 21 (2), pp. 145-55.
14. J.A. Duffy and M.D. Ingram: *J. Am. Chem. Soc.*, 1971, vol. 93, pp. 6448-55.
15. C.B. Fincham and F.D. Richardson: *Proc. R. Soc. A*, 1954, vol. 223, pp. 40-62.
16. K.P. Abraham and F.D. Richardson: *J. Iron Steel Inst.*, 1960, vol. 196, pp. 309-17.
17. K. Kärsrud: *Scand. J. Metall.*, 1984, vol. 13, pp. 144-50.